

Cite this: *Phys. Chem. Chem. Phys.*, 2012, **14**, 720–729

www.rsc.org/pccp

PAPER

# Crossed beam reaction of phenyl and D5-phenyl radicals with propene and deuterated counterparts—competing atomic hydrogen and methyl loss pathways

R. I. Kaiser,<sup>\*a</sup> D. S. N. Parker,<sup>a</sup> M. Goswami,<sup>a</sup> F. Zhang,<sup>a</sup> V. V. Kislov,<sup>b</sup>  
A. M. Mebel,<sup>\*b</sup> J. Aguilera-Iparraguirre<sup>c</sup> and W. H. Green<sup>c</sup>

Received 29th August 2011, Accepted 31st October 2011

DOI: 10.1039/c1cp22758k

We conducted the crossed molecular beams reactions of the phenyl and D5-phenyl radicals with propylene together with its partially deuterated reactants at collision energies of  $\sim 45$  kJ mol<sup>-1</sup> under single collision conditions. The scattering dynamics were found to be indirect and were mainly dictated by an addition of the phenyl radical to the sterically accessible CH<sub>2</sub> unit of the propylene reactant. The resulting doublet radical isomerized to multiple C<sub>9</sub>H<sub>11</sub> intermediates, which were found to be long-lived, decomposing in competing methyl group loss and atomic hydrogen loss pathways with the methyl group loss leading to styrene (C<sub>6</sub>H<sub>5</sub>C<sub>2</sub>H<sub>3</sub>) and the atomic hydrogen loss forming C<sub>9</sub>H<sub>10</sub> isomers *cis/trans* 1-phenylpropene (CH<sub>3</sub>CHCHC<sub>6</sub>H<sub>5</sub>) and 3-phenylpropene (C<sub>6</sub>H<sub>5</sub>CH<sub>2</sub>C<sub>2</sub>H<sub>3</sub>). Fractions of the methyl *versus* hydrogen loss channels of  $68 \pm 16\% : 32 \pm 10\%$  were derived experimentally, which agrees nicely with RRKM theory. As the collision energy rises to 200 kJ mol<sup>-1</sup>, the contribution of the methyl loss channel decreases sharply to typically 25%; the decreased importance of the methyl group loss channel was also demonstrated in previous crossed beam experiments conducted at elevated collision energies of 130–193 kJ mol<sup>-1</sup>. The presented work highlights the interesting differences of the branching ratios with rising collision energies in the reaction dynamics of phenyl radicals with unsaturated hydrocarbons related to combustion processes. The facility of forming styrene, a common molecule found in combustion against the elusiveness of forming the cyclic indane molecule demonstrates the need to continue to explore the potential surfaces through the combinative single collision experiment and electronic structure calculations.

## 1. Introduction

During recent years, the C<sub>9</sub>H<sub>10</sub> potential energy surface (PES) has received considerable attention from the experimental, theoretical, and combustion chemistry communities, since C<sub>9</sub>H<sub>10</sub> isomers like the aromatic and bicyclic indane molecule as well as its  $\alpha$ -methylstyrene (2-phenylpropene) and *cis/trans*-1-phenylpropene isomers are considered as important reaction intermediates and toxic byproducts in the combustion of fossil fuel.<sup>1–10</sup> Recent kinetic models<sup>1,6,11</sup> suggest that the aromatic phenyl radical, C<sub>6</sub>H<sub>5</sub>(X<sup>2</sup>A<sub>1</sub>), represents a crucial building block to yield the second ring and initiates the formation of polycyclic aromatic hydrocarbons (PAHs) and related molecules such as (partially) hydrogenated and/or dehydrogenated

PAHs in combustion flames and in combustion engines. Previous experiments of the phenyl radical with unsaturated hydrocarbons ranging from acetylene<sup>12</sup> *via* 1,3-butadiene<sup>13</sup> to benzene<sup>14</sup> conducted under single collision conditions indicated that the phenyl radical adds with its radical center to the unsaturated bond (carbon–carbon double or triple bond) yielding doublet radical intermediates. At elevated collision energies of 71–185 kJ mol<sup>-1</sup>, these reaction intermediates were predominantly found to be short lived, undergo isomerization, and hence cyclization<sup>15</sup> to form PAHs. With respect to the phenyl–propylene system,<sup>16</sup> the chemical dynamics inferred from the center-of-mass translational and angular distributions suggested that the reaction was indirect and initiated by an addition of the phenyl radical to the C1-carbon atom of the propylene molecule at the =CH<sub>2</sub> unit to form a radical intermediate (CH<sub>3</sub>CHCH<sub>2</sub>C<sub>6</sub>H<sub>5</sub>) on the doublet surface. The lifetime of this intermediate was estimated to be about 0.4–1.0 of its rotational period. Additional investigations with D6-propylene specified that only a deuterium atom was emitted; the phenyl group was found to stay intact.

<sup>a</sup> Department of Chemistry, University of Hawaii at Manoa, Honolulu, HI 96822, USA

<sup>b</sup> Department of Chemistry and Biochemistry, Florida International University, Miami, FL 33199, USA

<sup>c</sup> Department of Chemical Engineering, Massachusetts Institute of Technology, Cambridge, MA 02139, USA

**Table 1** Peak velocities ( $v_p$ ), speed ratios ( $S$ ), center-of-mass angles ( $\Theta_{CM}$ ), and the collision energies of the phenyl radical with the reactants ( $E_c$ ) of the segments crossing at the interaction region

Beam	$v_p$ , $\text{ms}^{-1}$	$S$	$E_c$ , $\text{kJ mol}^{-1}$	$\Theta_{CM}$
$\text{C}_6\text{H}_5(\text{X}^2\text{A}_1)/\text{He}$	$1667 \pm 17$	$9.1 \pm 0.6$	—	—
$\text{CH}_3\text{CHCH}_2(\text{X}^1\text{A}')/\text{He}$	$815 \pm 20$	$7.8 \pm 1.0$	$44.7 \pm 2.4$	$14.8 \pm 1.0$
$\text{C}_6\text{D}_5(\text{X}^2\text{A}_1)/\text{He}$	$1694 \pm 16$	$9.3 \pm 0.7$	—	—
$\text{CH}_3\text{CHCH}_2(\text{X}^1\text{A}')/\text{He}$	$815 \pm 20$	$7.8 \pm 1.0$	$47.0 \pm 2.3$	$14.6 \pm 0.9$
$\text{C}_6\text{D}_5(\text{X}^2\text{A}_1)/\text{He}$	$1620 \pm 16$	$9.5 \pm 0.7$	—	—
$\text{CD}_3\text{CHCH}_2(\text{X}^1\text{A}')/\text{He}$	$815 \pm 20$	$7.8 \pm 1.0$	$44.5 \pm 1.9$	$14.0 \pm 0.9$
$\text{C}_6\text{D}_5(\text{X}^2\text{A}_1)/\text{He}$	$1656 \pm 16$	$7.7 \pm 0.7$	—	—
$\text{CH}_3\text{CDCD}_2(\text{X}^1\text{A}')/\text{He}$	$815 \pm 20$	$7.8 \pm 1.0$	$46.6 \pm 2.0$	$15.1 \pm 0.9$
$\text{C}_6\text{H}_5(\text{X}^2\text{A}_1)/\text{He}$	$1663 \pm 13$	$8.7 \pm 0.6$	—	—
$\text{CD}_3\text{CDCD}_2(\text{X}^1\text{A}')/\text{He}$	$815 \pm 20$	$7.8 \pm 1.0$	$48.3 \pm 2.2$	$15.9 \pm 1.0$

Studies with 1,1,2-D3- and 3,3,3-D3-propylene indicated that the initial collision complexes  $\text{CH}_3\text{CDCD}_2\text{C}_6\text{H}_5$  (from 1,1,2-D3-propylene) and  $\text{CD}_3\text{CHCH}_2\text{C}_6\text{H}_5$  (from 3,3,3-D3-propylene) eject both a hydrogen atom *via* rather loose exit transition state to form the D3-isotopomers of *cis/trans*-1-phenylpropene ( $\text{CH}_3\text{CHCHC}_6\text{H}_5$ ) and 3-phenylpropene ( $\text{H}_2\text{CCHCH}_2\text{C}_6\text{H}_5$ ), respectively. The methyl group loss forming styrene ( $\text{C}_6\text{H}_5\text{C}_2\text{H}_3$ ) was not monitored due to the unfavorable kinematics combined with low signal-to-noise, the low intensity of the pyrolytically generated phenyl radical beam, and/or due to the low branching ratio of this channel at elevated collision energies. Note that previous studies of the phenyl-propylene system in liquid propylene at 183 K utilizing electron spin resonance also concluded that the reaction is initiated by an addition of the phenyl radical to the C1-carbon atom of propylene.<sup>16</sup> However, in the liquid phase, the authors also provided evidence for the existence of the  $\text{C}_6\text{H}_5\text{CH}_3\text{CHCH}_2$  radical formed *via* addition of phenyl to the C2-carbon atom of propylene and the allyl radical as an abstraction product. Recently, a kinetics study by Park *et al.* utilizing cavity ring-down spectroscopy at temperatures between 296 and 496 K, and *ab initio* calculations<sup>17</sup> concluded that the phenyl radical adds preferentially to the C1 carbon atom of the propylene molecule. However, reaction products were elusive in that study due to the lack of product detection schemes.

Here, we present new data on the crossed molecular beams reactions of photolytically generated phenyl and D5-phenyl radicals with propylene and its partially deuterated isotopologues to elucidate the formation of  $\text{C}_9\text{H}_{10}$  isomers at lower collision energies less than  $49 \text{ kJ mol}^{-1}$  in an attempt to increase the lifetime of the reaction intermediate(s) and hence to trigger a potential ring closure, and indane formation. Further, the almost ten-fold enhanced intensity of the photolytically generated phenyl radical beam (*cf.* section 2) compared to the pyrolytic source<sup>13</sup> employed previously in our laboratory allows us to reinvestigate the methyl radical loss pathway to styrene at a lower collision energy than conducted previously.<sup>13</sup> Finally, we combine these experimental studies with electronic structure and statistical rate constants/branching ratios calculations to get a deeper insight into the reaction mechanism. Eventually, we intend to utilize these results in kinetic flame modeling with the goal not only to elucidate the formation of  $\text{C}_9\text{H}_{10}$  isomers in the primary phenyl plus propylene reaction, but also to reveal how these isomers can undergo successive hydrogen abstractions followed by atomic hydrogen elimination

thus accessing the  $\text{C}_9\text{H}_8$  surface with its prominent indene structure as detected in combustion flames.<sup>1,3-7</sup>

## 2. Experimental

Our experiments were conducted under single collision conditions in a crossed molecular beams machine at the University of Hawaii.<sup>18</sup> Briefly, a helium-seeded molecular beam of (deuterated) phenyl radicals ( $\text{C}_6\text{H}_5$ ,  $\text{C}_6\text{D}_5$ ;  $\text{X}^2\text{A}_1$ ) at fractions of about 1% was prepared by photolysis of (deuterated) chlorobenzene ( $\text{C}_6\text{H}_5\text{Cl}$  99.9%;  $\text{C}_6\text{D}_5\text{Cl}$  99%; Fluka) in the primary source. The mixture of the helium carrier gas and (deuterated) chlorobenzene vapor was introduced to the piezoelectric pulsed valve (Proch-Trickl) operated at 120 Hz and a backing pressure of about 1.5 atm. The (deuterated) chlorobenzene was photolyzed by focusing the 193 nm excimer laser output operating at 60 Hz and 10 mJ per pulse 1 mm downstream of the nozzle prior to the skimmer without a Teflon extension channel. Under our experimental conditions, the photolysis of chlorobenzene in the part of the beam intersected by the laser was estimated to be about 90% using a  $1 \times 3 \text{ mm}$  focal region with an absorption cross section of  $9.6 \times 10^{-18} \text{ cm}^2$  at 193 nm.<sup>19</sup> The molecular beam entraining the (deuterated) phenyl radical passed a skimmer and a four-slot chopper wheel, which selected segments of the pulsed (deuterated) phenyl radical ( $\text{C}_6\text{D}_5$ ,  $\text{X}^2\text{A}_1$ ) beam of well-defined peak velocities ( $v_p$ ) and speed ratios ( $S$ ) (Table 1). The speed ratio is the velocity spread of the beam expressed as,  $S = v_p/(m/2k_B T)^{1/2}$ , where  $T$  is the temperature of the beam,  $m$  is the mass and  $k_B$  is the Boltzmann distribution. It should be stressed that the photolytic source produces phenyl radical beams with lower peak velocities compared to our pyrolytic source thus resulting in reduced collision energies with the co-reactant; at the same time, number densities are about one order of magnitude higher compared to those obtained from the pyrolysis source utilized in previous experiments in our group.<sup>16</sup> The phenyl radical beam bisected a pulsed molecular beam of the neat hydrocarbon generated in the secondary source with a pulsed valve at a backing pressure of 550 Torr fired 20  $\mu\text{s}$  prior to the pulsed valve in the primary source (Table 1). We utilized the following hydrocarbon reactants: propylene ( $\text{CH}_3\text{CHCH}_2$ , Aldrich; 99+%), D6-propylene ( $\text{CD}_3\text{CDCD}_2$ , CDN; 99+ % D), 3,3,3-D3-propylene ( $\text{CD}_3\text{CHCH}_2$ , CDN; 99+ % D), and 1,1,2-D3-propylene ( $\text{CH}_3\text{CDCD}_2$ , CDN; 99+ % D). The reaction products were monitored using a triply differentially pumped quadrupole mass spectrometer (QMS) in the time-of-flight (TOF) mode after electron-impact ionization of the neutral molecules at 80 eV with an emission current of 2 mA. The ions were separated according to their mass-to-charge ratio by an Extrel QC 150 quadrupole mass spectrometer operated with an oscillator at 1.2 MHz; only ions with the desired mass-to-charge,  $m/z$ , value passed through and were accelerated toward a stainless steel 'door knob' target coated with an aluminum layer and operated at a voltage of  $-22.5 \text{ kV}$ . The ions hit the surface and initiated an electron cascade that was accelerated by the potential until they reached an aluminum coated organic scintillator whose photon cascade was detected by a photomultiplier tube (PMT, Burle, Model 8850, operated at  $-1.35 \text{ kV}$ ). The signal from the PMT was then filtered by a discriminator

(Advanced Research Instruments, Model F-100TD, level: 1.6 mV) prior to feeding into a Stanford Research System SR430 multi-channel scaler to record time-of-flight spectra.<sup>20,21</sup> The TOF spectra recorded at each angle and the product angular distribution in the laboratory frame (LAB) were fit with Legendre polynomials using a forward-convolution routine.<sup>22</sup> This method uses an initial choice of the product translational energy  $P(E_T)$  and the angular distribution  $T(\theta)$  in the center-of-mass reference frame (CM) to reproduce TOF spectra and a product angular distribution. The TOF spectra and product angular distribution obtained from the fit were then compared to the experimental data. The parameters of the  $P(E_T)$  and  $T(\theta)$  were iteratively optimized until the best fit was reached. Branching ratios were calculated using the method elucidated in the literature.<sup>23</sup>

### 3. Theoretical

To map out the potential energy surface for the phenyl radical + propylene reaction we utilized DFT B3LYP<sup>24–27</sup> method combined with a modified G3(MP2,CC)//B3LYP<sup>28,29</sup> approach for high-level single-point energy calculations. Geometries of all local minima and transition states were fully optimized at the B3LYP/6-311G(d,p) level, and the same method was used to compute vibrational frequencies, zero-point energy (ZPE) corrections and molecular structural parameters required for subsequent statistical calculations of reaction rate constants. Energies of all species were then refined using the G3(MP2,CC)//B3LYP<sup>28,29</sup> modification of the original Gaussian 3 (G3) scheme.<sup>30</sup> The final energies at 0 K were obtained using the B3LYP optimized geometries and ZPE corrections according to the following formula

$$E_0[\text{G3(MP2,CC)}] \\ = E[\text{RHF-RCCSD(T)/6-311G(d,p)}] \\ + \Delta E_{\text{MP2}} + \Delta E(\text{SO}) + \Delta E(\text{HLC}) + E(\text{ZPE}),$$

where  $\Delta E_{\text{MP2}} = E[\text{MP2/G3large}] - E[\text{MP2/6-311G(d,p)}]$  is the basis set correction,  $\Delta E(\text{SO})$  is a spin-orbit correction (not included in our calculations),  $\Delta E(\text{HLC})$  is a higher level correction, and  $E(\text{ZPE})$  is the zero-point energy.  $\Delta E(\text{HLC})$  was omitted in the present calculations because in most cases isomerizations of radical species considered here proceed without a spin change, resulting in HLC cancellation. Otherwise, a neglect of HLC normally introduces an error of about 10 kJ mol<sup>-1</sup>. The GAUSSIAN 98<sup>31</sup> program package was used to carry out B3LYP and MP2 calculations, and the MOLPRO 2006<sup>32</sup> program package was employed to perform calculations of spin-restricted coupled clusters energies RHF-RCCSD(T). Also, we applied microcanonical Rice-Ramsperger-Kassel-Marcus (RRKM) theory<sup>33–35</sup> to calculate energy-dependent reaction rate constants for all individual reaction steps relevant to single-collision conditions, with collision energies varied within 0–200 kJ mol<sup>-1</sup> covering the experimental conditions and beyond. For unimolecular reactions on the C<sub>9</sub>H<sub>11</sub> surface, the collision energy was added to the energy of chemical activation in the phenyl plus propylene reaction to obtain the total available internal energy for each species. To compute rate constants for two barrierless H-elimination steps (**i15** → **p6** + H, and **i24** → **p7** + H), we utilized microcanonical variational transition state

theory (VTST).<sup>34</sup> Harmonic approximation was used for the calculations of numbers and densities of states, except the low-frequency torsional motions were treated as hindered rotors. The RRKM and VTST calculated rate constants were further utilized to compute relative product yields using the steady-state approximation.

## 4. Results

### 4.1. Laboratory data

For the phenyl-propylene system, reactive scattering signal was first recorded at mass-to-charge ratios of  $m/z = 118$  (C<sub>9</sub>H<sub>10</sub><sup>+</sup>) (Fig. 1) and  $m/z = 117$  (C<sub>9</sub>H<sub>9</sub><sup>+</sup>). The time-of-flight spectra recorded at the lower  $m/z$  ratios depicted, after scaling, an identical pattern and were fit with identical center-of-mass functions as those data taken at  $m/z = 118$ . This finding indicates that signal at  $m/z = 117$  originated from dissociative ionization of the C<sub>9</sub>H<sub>10</sub> parent molecule in the electron impact ionizer of the detector. Further, we can conclude that in the reaction of the phenyl radical with propylene, the phenyl *versus* atomic hydrogen pathway is open, but the molecular hydrogen elimination pathway to form C<sub>9</sub>H<sub>9</sub> is closed. Besides the atomic hydrogen loss, we also scanned for the methyl group (CH<sub>3</sub>) loss channel with C<sub>8</sub>H<sub>8</sub> isomer(s) as the heavy co-fragment (Fig. 2). Therefore, we monitored ion counts at  $m/z = 104$  (C<sub>8</sub>H<sub>8</sub><sup>+</sup>); these TOF spectra were, after scaling, not superimposable to those recorded at  $m/z = 118$  (C<sub>9</sub>H<sub>10</sub><sup>+</sup>). Hence, we can conclude that under our experimental conditions the kinetically less favorable methyl loss pathway is accessible. Note that for completeness, we could confirm that signal at  $m/z = 119$  originated from <sup>13</sup>C-substituted C<sub>9</sub>H<sub>10</sub> isomer(s), *i.e.* <sup>13</sup>CC<sub>8</sub>H<sub>10</sub><sup>+</sup>, which are formed at fractions of about 10% due to the naturally occurring <sup>13</sup>C isotope. The corresponding laboratory angular distributions for the atomic hydrogen and methyl loss pathways are depicted in Fig. 3 and 4 for ions at  $m/z = 118$  (C<sub>9</sub>H<sub>10</sub><sup>+</sup>) and  $m/z = 104$  (C<sub>8</sub>H<sub>8</sub><sup>+</sup>), respectively. As expected from an atomic hydrogen loss and the mass of the heavy reaction product, the LAB distribution is narrow (Fig. 3), peaks close to the center-of-mass angle (Table 1), is within the error limits forward-backward symmetric, and spreads only over about 16° in the scattering plane defined by both supersonic beams. Based on energy and momentum conservation, the C<sub>8</sub>H<sub>8</sub> product formed during the methyl

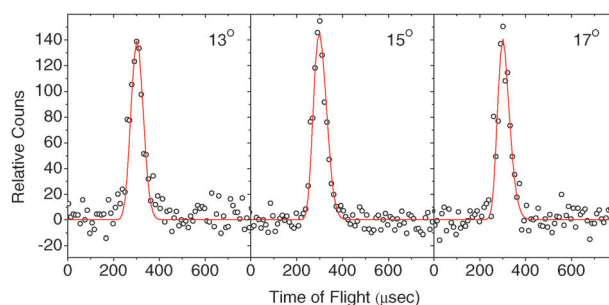


**Fig. 1** Time-of-flight data for the reaction of the phenyl radical, C<sub>6</sub>H<sub>5</sub>(X<sup>2</sup>A<sub>1</sub>), with propylene, CH<sub>3</sub>CHCH<sub>2</sub>(X<sup>1</sup>A'), monitored at  $m/z = 118$  (C<sub>9</sub>H<sub>10</sub><sup>+</sup>). The circles present the experimental data, the line utilizing the best fit center-of-mass functions.

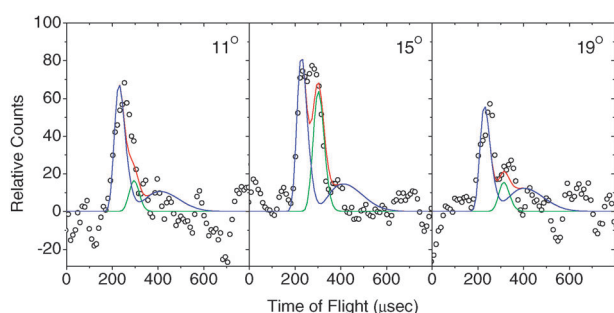


**Fig. 2** Time-of-flight data for the reaction of the phenyl radical,  $C_6H_5(X^2A_1)$ , with propylene,  $CH_3CHCH_2(X^1A')$ , monitored at  $m/z = 104$  ( $C_8H_8^+$ ). The circles present the experimental data. The green and blue lines represent the fits derived from the  $C_9H_{10} + H$  (dissociative electron impact ionization of  $C_9H_{10}$  to  $C_8H_8^+$ ) and the  $C_8H_8 + CH_3$  channels ( $C_8H_8^+$ ), respectively, whereas the red line presents the sum.

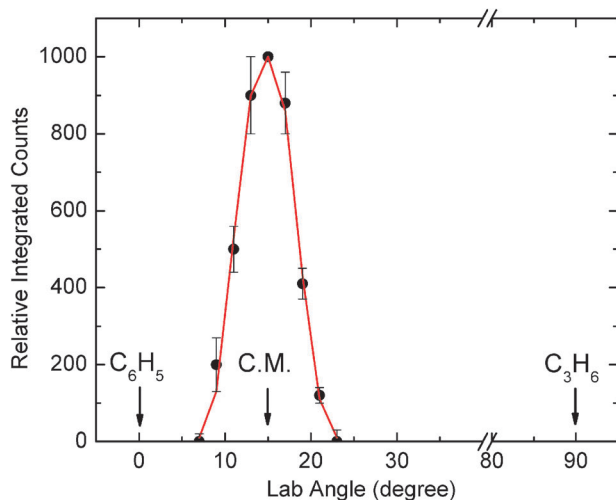


**Fig. 3** Laboratory angular distribution of the  $C_9H_{10}$  reaction product formed in the reaction of phenyl plus propylene recorded at  $m/z = 118$  ( $C_9H_{10}^+$ ). The circles present the experimental data, the red line the fits utilizing the best fit center-of-mass functions. C.M. designates the center-of-mass angle.

elimination is expected to be scattered over a larger scattering range of about  $30^\circ$  (Fig. 4).

Similar to the reaction of phenyl with propylene conducted at collision energies between 130 and 194  $\text{kJ mol}^{-1}$ , we also collected data on the position of the hydrogen loss (phenyl versus methyl group versus vinyl hydrogen atoms). First, we carried out the reaction of D5-phenyl radical ( $C_6D_5$ ) with propylene and investigated reactive scattering signal at  $m/z = 123$  ( $C_9H_5D_5^+$ ), i.e. an atomic hydrogen loss from the propylene molecule (Fig. 5). This study could clearly verify signal at  $m/z = 123$  ( $C_9H_5D_5^+$ ), therefore providing evidence that the hydrogen atom is at least emitted from the propylene molecule. The corresponding TOFs and LAB distributions are depicted in Fig. 5 and 6, respectively. However, we point out that the hydrogen atom can be released either from the vinyl or from the methyl group of the propylene molecule (or from both). To elucidate the ultimate pathway(s), we carried out crossed beam experiments of phenyl radicals with 3,3,3-D3-propylene

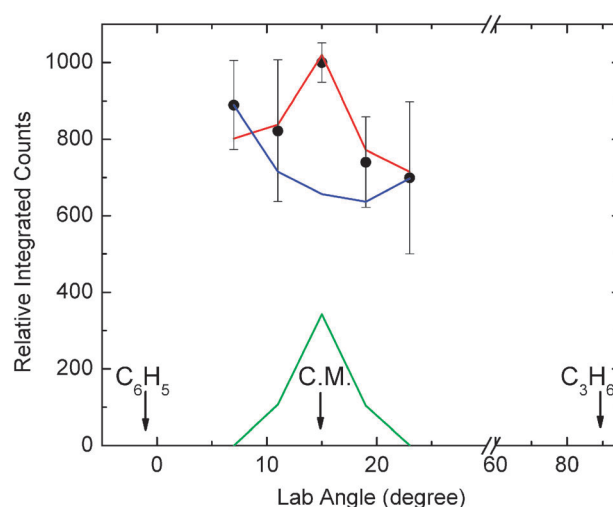


**Fig. 4** Laboratory angular distribution of  $C_8H_8^+$  recorded at  $m/z = 104$  in the reaction of phenyl with propylene. The circles present the experimental data. The green and blue lines represent the fits derived from the  $C_9H_{10} + H$  (dissociative electron impact ionization of  $C_9H_{10}$  to  $C_8H_8^+$ ) and the  $C_8H_8 + CH_3$  channels ( $C_8H_8^+$ ), respectively, whereas the red line presents the sum. C.M. designates the center-of-mass angle.

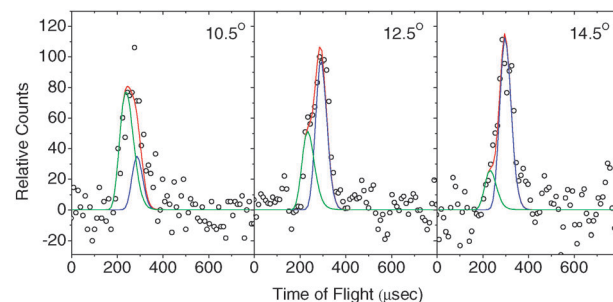


**Fig. 5** Time-of-flight data for the reaction of the D5-phenyl radical ( $C_6D_5$ ,  $X^2A_1$ ) with propylene  $CH_3CHCH_2(X^1A')$  monitored at  $m/z = 123$  ( $C_9H_5D_5^+$ ). The circles present the experimental data, the blue lines the fits. The green lines present a non-reactively scattered contribution to  $m/z = 123$  from the primary beam. The red line presents the sum.

( $CD_3CHCH_2$ ) and 1,1,2-D3-propylene ( $CH_3CDCD_2$ ). For the phenyl-3,3,3-D3-propylene reaction, if a hydrogen atom is emitted from the vinyl group, signal must be detectable at  $m/z = 121$  ( $C_9H_7D_3^+$ ); if a deuterium atom ejection takes place, ion counts at  $m/z = 120$  ( $C_9H_8D_2^+$ ) should be traceable. Also, signal at  $m/z = 120$  can arise from fragmentation of  $C_9H_7D_3^+$ . On the other hand, let us analyze the 1,1,2-D3-propylene reactant. If atomic hydrogen is emitted from the methyl group, signal should be monitored at  $m/z = 121$  ( $C_9H_7D_3^+$ ); however, if an atomic deuterium is released from the vinyl group, we should probe ion counts at  $m/z = 120$  ( $C_9H_8D_2^+$ ). Similar to the reaction of phenyl radicals with 3,3,3-D3-propylene, signal at  $m/z = 120$  may originate from fragmentation of  $C_9H_7D_3^+$ . Therefore, if signal at  $m/z = 121$  is observed during the reactions of phenyl radicals with 3,3,3-D3-propylene and 1,1,2-D3-propylene, it should be a unique indicator of a hydrogen atom loss from the vinyl and methyl

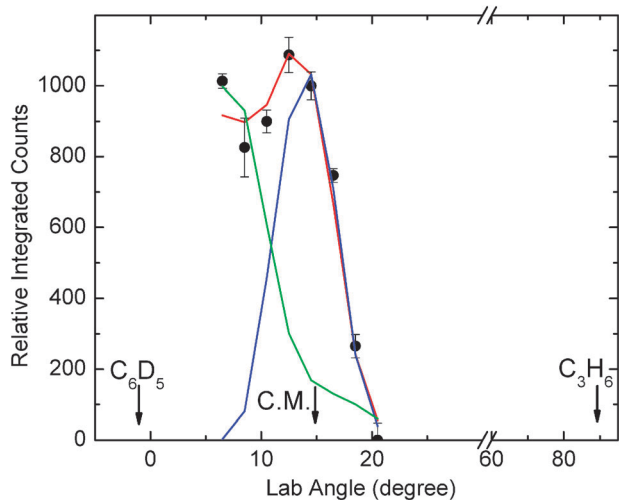


**Fig. 6** Laboratory angular distribution recorded at  $m/z$  123 in the reaction of D5-phenyl with propylene. The circles present the experimental data, the red line the fits utilizing the best fit center-of-mass functions. The blue and green lines present the fits for the reactive and non-reactive channels, respectively, whereas the red line presents the sum. C.M. designates the center-of-mass angle.

groups, respectively. In our experiments, we monitored signal at  $m/z = 121$  for the 3,3,3-D3-propylene and 1,1,2-D3-propylene reactants (Fig. 7). Therefore, we can conclude that two hydrogen elimination pathways exist: from the vinyl group and from the methyl group. Finally, we conducted the reaction of the phenyl radical ( $C_6H_5$ ) with D6-propylene and monitored the TOF spectra at the center-of-mass angle (Table 1). In the case of a hydrogen atom ejection, signal should be observable at  $m/z = 124$  ( $C_9H_4D_6^+$ ); if a deuterium atom elimination happens, we would monitor ion counts at  $m/z = 123$  ( $C_9H_5D_5^+$ ). Note that  $m/z = 123$  may also originate from fragmentation of  $m/z = 124$ . In our experiment, we had no conclusive evidence of the atomic hydrogen loss pathway; signal at  $m/z = 124$  was observed, but at levels consistent with the existence of  $^{13}C$  labeled products ( $^{13}CC_8H_5D_5^+$ ). Note also that experiments with perdeuterated and partially deuterated reactants only allowed us to record TOF spectra at the center-of-mass angles due to the low signal counts and the costs of the chemicals (Table 1).

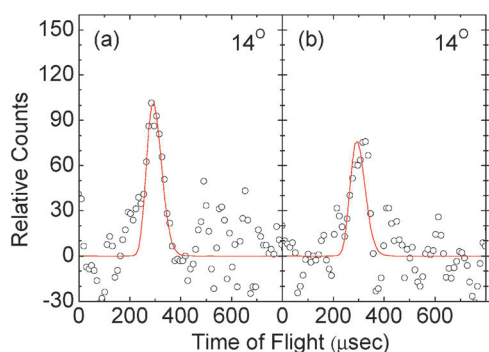


**Fig. 7** Center-of-mass time-of-flight data for the atomic hydrogen loss pathway in the reactions of the phenyl radical ( $C_6H_5$ ,  $X^2A_1$ ) with partially deuterated propylenes  $CD_3CHCH_2(X^1A')$  (a) and  $CH_3CDCD_2(X^1A')$  (b) monitored at  $m/z = 121$  ( $C_9H_7D_3^+$ ).

#### 4.2. Center of mass translational energy, $P(E_T)$ , and angular distributions, $T(\theta)$

The corresponding center-of-mass functions for the phenyl-propylene and D5-phenyl-propylene reactions are shown in Fig. 8 (hydrogen atom loss), Fig. 9 (methyl loss), and Fig. 10 (hydrogen atom loss), respectively. As evident from the center-of-mass functions for the atomic hydrogen loss pathways (Fig. 8 and 10), a reasonable fit of the TOF data and LAB distributions of both reactions could be achieved with a single reaction channel by utilizing essentially identical translational energy and angular center-of-mass functions leading to atomic hydrogen elimination. Best fits of the center-of-mass translational energy distributions,  $P(E_T)$ s, were achieved with distributions extending to maximum translational energy releases,  $E_{max}$ , of about 60–80  $\text{kJ mol}^{-1}$ . This high energy cutoff resembles the sum of the absolute of the reaction energy plus the collision energy suggesting that the reaction leading to  $C_9H_{10}/C_9D_5H_5$  plus atomic hydrogen is exoergic by about  $24 \pm 11 \text{ kJ mol}^{-1}$ . Also, the  $P(E_T)$ s present distribution maximum at 20–30  $\text{kJ mol}^{-1}$ , indicating the existence of tight exit transition states. Further, the fractions of available energy channeling into the translations degrees of freedom of the products were calculated to be  $38 \pm 15\%$ . On the other hand, the laboratory data of the methyl loss pathway (Fig. 2 and 4) could be fit only with two channels, *i.e.* dissociative ionization of the  $C_9H_{10}$  parent molecule in the ionizer and from the ionized  $C_8H_8$  molecule formed in the methyl loss pathway. The corresponding translational energy distribution holds a high energy cutoff of 105–133  $\text{kJ mol}^{-1}$  suggesting that—after a subtraction of the collision energy, the reaction is exoergic by about  $74 \pm 14 \text{ kJ mol}^{-1}$ . Further, the distribution peaks away from zero translational energy suggesting a tight exit transition state as well. Finally, the

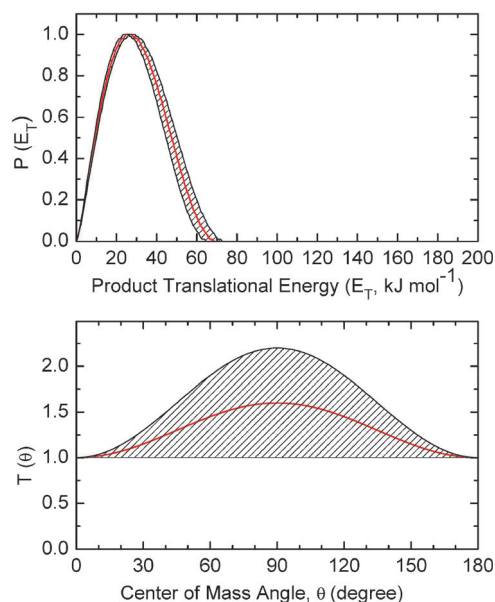


**Fig. 8** Center-of-mass translational energy flux distribution (upper) and angular distribution (lower) for the hydrogen atom loss pathway(s) in the phenyl-propylene system. Hatched areas indicate the acceptable upper and lower error limits of the fits and the solid red line defines the best-fit function.

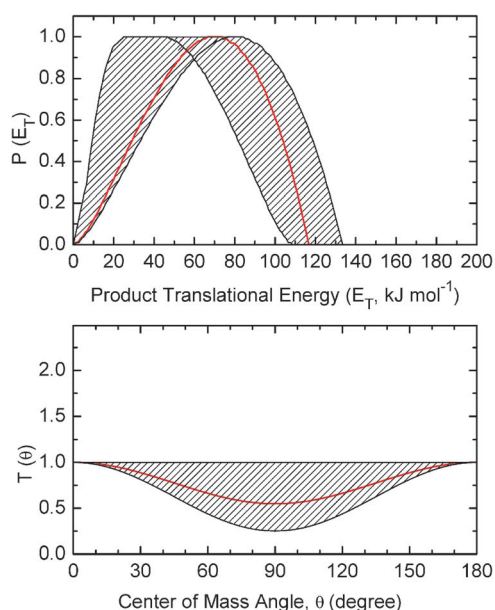


**Fig. 9** Center-of-mass translational energy flux distribution (upper) and angular distribution (lower) for the methyl group loss in the phenyl-propylene system. Hatched areas indicate the acceptable upper and lower error limits of the fits and the solid red line defines the best-fit function.

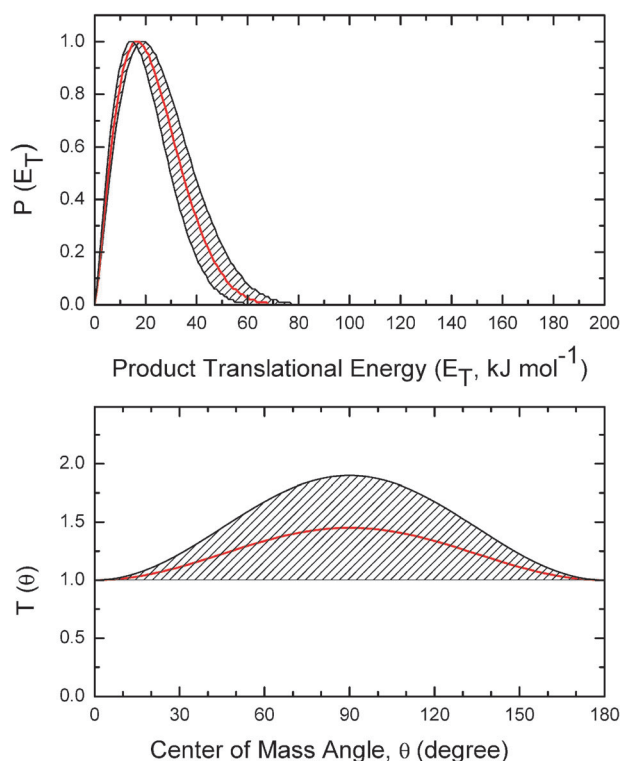


**Fig. 10** Center-of-mass translational energy flux distribution (upper) and angular distribution (lower) for the atomic hydrogen loss in the D5-phenyl-propylene system. Hatched areas indicate the acceptable upper and lower error limits of the fits and the solid red line defines the best-fit function.

averaged fraction of energy channeling into the translational modes of the products was estimated to be  $55 \pm 20\%$ .

The center-of-mass angular distributions help to gather further information on the reaction dynamics. Here, the angular flux

distributions of the hydrogen loss channels (Fig. 8 and 10) are forward-backward symmetric around  $90^\circ$  and depict intensity over the complete angular range from  $0^\circ$  to  $180^\circ$ . These data suggest that the reaction follows indirect scattering dynamics *via* formation of  $C_9H_{11}/C_9H_6D_5$  complexes with lifetimes longer than their rotation periods.<sup>35</sup> Further, best fits were obtained with functions showing pronounced maxima at  $90^\circ$ ; however, within the error limits, isotropic distributions could also fit the experimental data. Due to the range of acceptable center-of-mass functions fitting the data from isotropic to functions with pronounced maxima, it is not a good idea to over-interpret the center-of-mass angular distributions of the atomic hydrogen loss channel. Considering the methyl loss pathway, the center-of-mass angular distribution is also forward-backward symmetric (indirect scattering dynamics; lifetime of the decomposing complex longer than the rotational period). However, best fits could be achieved with minima at  $90^\circ$ . This finding might suggest that the methyl group is emitted within the rotational plane of the decomposing complex.<sup>35</sup>

The branching ratio between the atomic hydrogen loss and the methyl loss channels were calculated to be  $32 \pm 10\% : 68 \pm 16\%$ , *i.e.* a dominating methyl group loss pathway at a collision energy of  $44.7 \pm 2.4 \text{ kJ mol}^{-1}$ .

## 5. Discussion

Before we interpret the experimental results and center of mass functions, we would like to compile the results to aid the following discussion.

R1. In the phenyl-propylene and D5-phenyl-propylene systems, we observed an atomic hydrogen loss channel to form  $C_9H_{10}$  and  $C_9H_5D_5$ , respectively. The center-of-mass functions for both systems are essentially identical suggesting reaction exoergies of about  $24 \pm 11 \text{ kJ mol}^{-1}$ , tight exit transition states, and indirect reaction dynamics *via* complexes with lifetimes longer than their rotational periods.

R2. We also observed the methyl loss pathway for the phenyl-propylene system leading to  $C_8H_8$  isomer(s) with a reaction exoergicity of about  $74 \pm 14 \text{ kJ mol}^{-1}$ , a tight exit transition state, indirect scattering dynamics involving a long-lived  $C_9H_{11}$  complex, and branching ratios of  $68 \pm 16\%$  methyl loss compared to  $32 \pm 10\%$  atomic hydrogen loss.

R3. In the phenyl-D6-propylene system, no compelling evidence for an atomic hydrogen loss was presented, indicating that the phenyl group is conserved, and that in the phenyl-propylene and D5-phenyl propylene systems, the hydrogen atom is emitted from the propylene reactant.

R4. In the phenyl-3,3,3-D3-propylene and phenyl-1,1,2-D3-propylene systems, we observed an atomic hydrogen loss from the vinyl *and* from the methyl group, respectively. Therefore, at least two exit channels are open.

To elucidate the underlying reaction dynamics and mechanisms involved for the formation of  $C_9H_{10}$  plus atomic hydrogen and  $C_8H_8$  plus methyl group, we are comparing the experimental data with electronic structure calculations on the  $C_9H_{11}$  potential energy surface. The calculated reaction network for two possible addition channels (phenyl addition to the CH and  $CH_2$  groups of propylene) involving all considered rearrangements and hydrogen atom and methyl group eliminations is

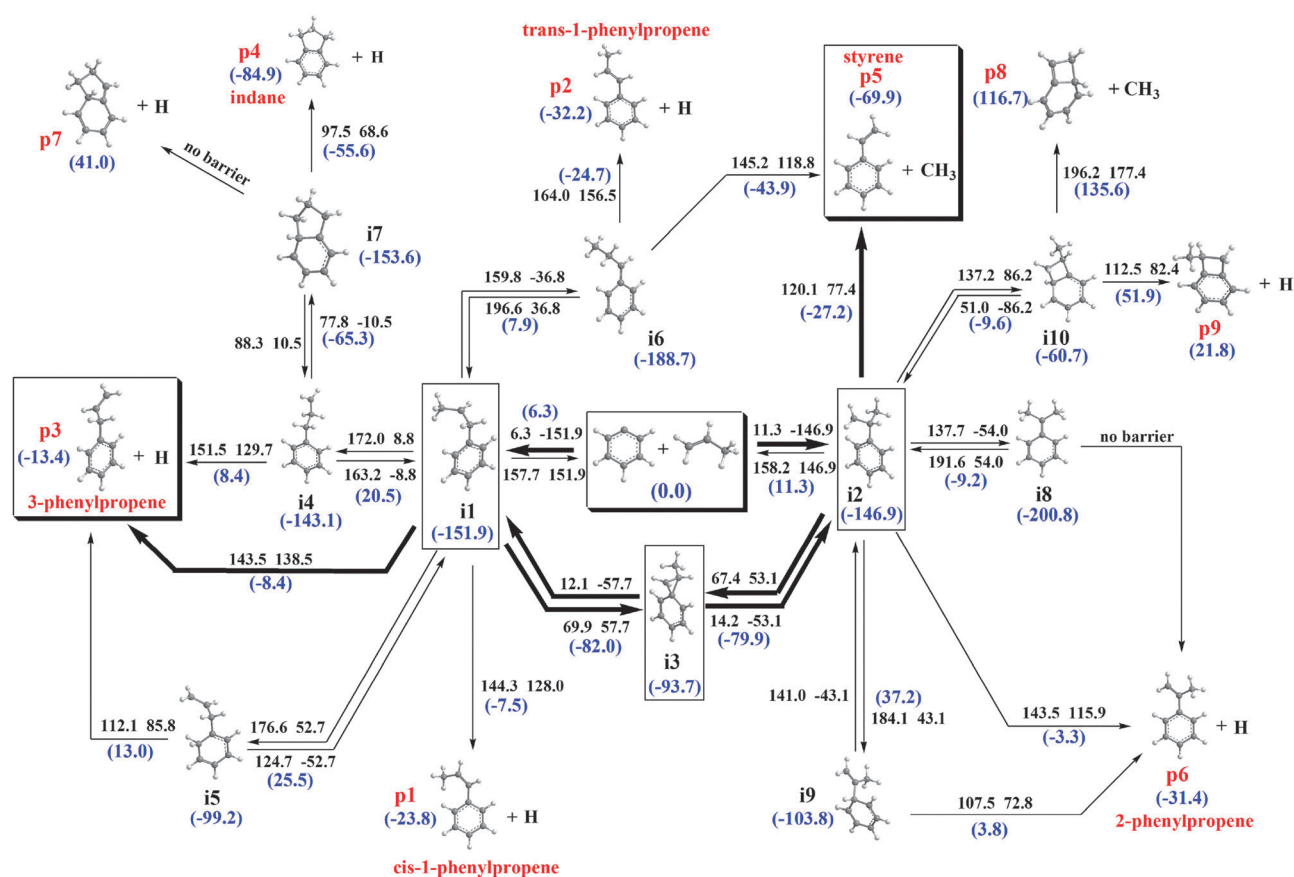


**Fig. 11** Potential energy diagram for the reactions of phenyl radicals with propylene forming  $C_9H_{10}$  and  $C_8H_8$  isomers. All relative energies (shown in blue color online and in parentheses, in  $\text{kJ mol}^{-1}$ ) are calculated at the G3(MP2,CC)//B3LYP/6-311G(d,p)+ZPE(B3LYP/6-311G(d,p)) level of theory. The numbers next to the arrows show the barrier (first) and the reaction energy (second) for each individual step in  $\text{kJ mol}^{-1}$ . The most important reaction pathways are highlighted by bold arrows and frames.

shown in Fig. 11 along with computed relative energies of all species (relative to reactants); barrier heights and reaction energies are also presented for each elementary reaction step in the network. It should be noted that three distinct direct H abstraction channels producing benzene plus  $C_3H_5$  radical isomers are also possible in this reaction, but we do not consider them here, as the products cannot be detected in the present experiment. The calculations suggest that the phenyl radical can add with its radical center to the C1 and/or C2 carbon atom of the propylene molecule forming intermediates **i1** and **i2**, respectively, *via* entrance barriers of 6 and 11  $\text{kJ mol}^{-1}$ , respectively. Both collision complexes can isomerize to each other *via* a formal phenyl group migration involving intermediate **i3**. Complex **i1** can either eject a hydrogen atom forming *cis*-1-phenylpropene ( $\text{CH}_3\text{CHCHC}_6\text{H}_5$ ; **p1**) or 3-phenylpropene ( $\text{CH}_2\text{CHCH}_2\text{C}_6\text{H}_5$ ; **p3**) *via* tight transition states located 16 and 5  $\text{kJ mol}^{-1}$  above the separated products, respectively; the overall reactions to form **p1** and **p3** products are exoergic by 24 and 13  $\text{kJ mol}^{-1}$ , respectively. 3-Phenylpropene **p3** can be also formed *via* two different two-step mechanisms in which the H loss is preceded by a hydrogen shift, one of them involving initial H migration in **i1** from  $\text{CH}_3$  to the neighboring CH group to form the **i4** intermediate with a barrier of 172  $\text{kJ mol}^{-1}$  and the second initiated by hydrogen migration from methyl to the aromatic ring producing **i5** *via* a 177  $\text{kJ mol}^{-1}$  barrier.

However, these migration barriers are respectively 28 and 33  $\text{kJ mol}^{-1}$  higher than the barrier for the hydrogen elimination **i1**  $\rightarrow$  **p3** + H. Alternatively, the **i1** adduct can isomerize *via* a  $\text{CH}_2$ -to- $\text{CH}$  hydrogen shift to the **i6** intermediate overcoming a barrier of 160  $\text{kJ mol}^{-1}$ , and **i6** can also emit a hydrogen atom producing *trans*-1-phenylpropene ( $\text{CH}_3\text{CHCHC}_6\text{H}_5$ ; **p2**) plus hydrogen atom *via* a barrier placed 7  $\text{kJ mol}^{-1}$  above the separated products (**p2** + H) or lose the methyl group *via* a tight exit transition state leading to styrene (**p5**) in a reaction with overall exoergic of 70  $\text{kJ mol}^{-1}$ . Note that **p5** plus methyl can also be accessed from intermediate **i2**. Finally, the **i4** intermediate formed from the initial collision complex **i1** after hydrogen migration can not only emit a hydrogen atom to yield 3-phenylpropene (**p3** + H), but also can ring close to form a bi-cyclic intermediate **i7**. Next, the ring closure can be followed by atomic hydrogen ejection giving two possible bicyclic aromatic products—indane **p4**, or its much less stable isomer **p7**. Both the **p4** and **p7** products possess an indene core, *i.e.* contain two fused six- and five-member rings, which means they can be considered as possible precursors of indene after being involved in secondary reactions (involving molecular hydrogen emission). The overall reaction energy to form indane plus a hydrogen atom was calculated to be  $-85 \text{ kJ mol}^{-1}$  with the barrier from **i7** to indane plus atomic hydrogen being  $98 \text{ kJ mol}^{-1}$ , whereas reaction to form **p7** plus a hydrogen atom from phenyl and

propylene is endoergic by  $41 \text{ kJ mol}^{-1}$ , and, in contrast to the  $\mathbf{i7} \rightarrow$  indane plus a hydrogen atom elimination, the hydrogen loss from  $\mathbf{i7}$  producing  $\mathbf{p7}$  exhibits no exit barrier, as confirmed by a careful PES scan.

Although phenyl radical addition to the C1 atom of propylene producing  $\mathbf{i1}$  complex is more kinetically favorable because its barrier is twice lower than that for the competitive formation of  $\mathbf{i2}$ , the alternative addition to C2 cannot be excluded from the consideration, especially at high collision energies/temperatures. Similarly to  $\mathbf{i1}$ , the  $\mathbf{i2}$  adduct can decompose *via* a one-step hydrogen loss from the vinyl group forming 2-phenylpropene ( $\text{C}_6\text{H}_5\text{CH}_3\text{CCH}_2$ ;  $\mathbf{p6}$ ) plus hydrogen atom with overall exothermicity of  $31 \text{ kJ mol}^{-1}$ . 2-phenylpropene  $\mathbf{p6}$  can be also accessed from  $\mathbf{i2}$  by two additional two-step pathways,  $\mathbf{i2} \rightarrow \mathbf{i8} \rightarrow \mathbf{p6} + \text{H}$  and  $\mathbf{i2} \rightarrow \mathbf{i9} \rightarrow \mathbf{p6}$  plus atomic hydrogen initiated by hydrogen atom migrations forming the  $\mathbf{i8}$  and  $\mathbf{i9}$  radical intermediates, respectively, with  $\mathbf{i8}$  being the lowest in energy among all species considered here. The  $\mathbf{i2} \rightarrow \mathbf{i9}$  hydrogen shift exhibits a barrier  $41 \text{ kJ mol}^{-1}$  higher than that for the instantaneous hydrogen atom ejection,  $\mathbf{i2} \rightarrow \mathbf{p6} + \text{H}$ , and therefore the formation of  $\mathbf{p6}$  *via* the  $\mathbf{i9}$  intermediate is not expected to be competitive with the direct one-step process. On the contrary, the  $\mathbf{i2} \rightarrow \mathbf{i8}$  hydrogen migration process exhibits a barrier  $6 \text{ kJ mol}^{-1}$  lower than that for the one-step hydrogen elimination and can contribute. Another alternative mechanism involving the  $\mathbf{i2}$  adduct is a four-member ring closure producing a bicyclic intermediate  $\mathbf{i10}$  which possesses fused four- and six-member rings. The barrier for the  $\mathbf{i2} \rightarrow \mathbf{i10}$  process is similar to those for the instantaneous hydrogen elimination  $\mathbf{i2} \rightarrow \mathbf{p6} + \text{H}$  and for the hydrogen migration  $\mathbf{i2} \rightarrow \mathbf{i8}$ , which allows it to be considered among competitive routes. However, both subsequent hydrogen atom loss producing  $\mathbf{p9} + \text{H}$  and methyl group elimination giving the  $\mathbf{p8} + \text{CH}_3$  products are overall endoergic by 22 and  $118 \text{ kJ mol}^{-1}$ , respectively, indicating that these products are not likely to be formed. The most energetically favorable mechanism involving  $\mathbf{i2}$  is direct elimination of the methyl group producing styrene  $\mathbf{p5}$  with the overall high exothermicity of  $70 \text{ kJ mol}^{-1}$  and the lowest barrier height among all considered dissociation pathways starting from  $\mathbf{i2}$ . This indicates that styrene is likely the major product formed from the  $\mathbf{i2}$  adduct, unless the  $\mathbf{i2} \rightarrow \mathbf{i3} \rightarrow \mathbf{i1}$  rearrangement of  $\mathbf{i2}$  to  $\mathbf{i1}$  affects the reaction kinetics significantly. This actually can be the case because the barriers on this pathway are much lower than those for any of the  $\mathbf{i1}$  and  $\mathbf{i2}$  fragmentation processes. Hence, the reactions of  $\mathbf{i2}$  need to be considered together with the processes involving  $\mathbf{i1}$ , in a common kinetic scheme.

In an attempt to untangle the actual reaction mechanism(s), we are comparing first the experimental reaction energies with the computed ones. For the atomic hydrogen loss channel, the experimentally derived reaction energy of  $-24 \pm 11 \text{ kJ mol}^{-1}$  (R1) correlates with the formation of  $\mathbf{p1}$ ,  $\mathbf{p2}$ , and/or  $\mathbf{p3}$ . The formation of the indane molecule seems unlikely, since computed reaction energy of  $-85 \text{ kJ mol}^{-1}$  cannot be confirmed by the experiments. This is also supported by the findings from the phenyl-D6-propylene system and the lack of an atomic hydrogen loss. Here, considering the reaction sequence  $\mathbf{i1} \rightarrow \mathbf{i4} \rightarrow \mathbf{i7} \rightarrow$  indane + H in the phenyl-D6-propylene system, intermediate  $\mathbf{i7}$  holds all hydrogen atoms at the former phenyl ring, and all

deuterium atoms at the former propylene moiety. Only a hydrogen atom loss from the bridged carbon atom belonging to the former phenyl moiety can yield indane. However, the lack of an observable atomic hydrogen loss in the reaction of phenyl with D6-propylene indicates that indane is only formed—if at all—in insignificant amounts. However, which of the products  $\mathbf{p1}$ ,  $\mathbf{p2}$ , and/or  $\mathbf{p3}$  is actually formed? Recall that in the phenyl-1,1,2-D3-propylene systems, we observed an atomic hydrogen loss from the methyl group. This process can only lead to D3-3-phenylpropene ( $\text{H}_2\text{CCDCD}_2\text{C}_6\text{H}_5$ ;  $\mathbf{p3}$ ) either in one step from  $\mathbf{i1}$  or *via*  $\mathbf{i4/i5}$ . Considering the barriers involved in the isomerization of  $\mathbf{i1}$  to  $\mathbf{i4}$  and  $\mathbf{i5}$  and in the decomposition of  $\mathbf{i1}$  to  $\mathbf{p3}$  plus atomic hydrogen (Fig. 11), the atomic hydrogen emission from  $\mathbf{i1}$  and hence formation of D3-3-phenylpropene ( $\text{H}_2\text{CCDCD}_2\text{C}_6\text{H}_5$ ;  $\mathbf{p3}$ ) should be favorable compared to the reaction sequences  $\mathbf{i1} \rightarrow \mathbf{i4/i5} \rightarrow \mathbf{p3} + \text{H}$ .

On the other hand, the experimental detection of the atomic hydrogen loss in the phenyl-3,3,3-D3-propylene reaction can be explained by the formation of *cis*- and/or *trans*-1-phenylpropene ( $\text{CD}_3\text{CHCHC}_6\text{H}_5$ ;  $\mathbf{p1/p2}$ ) from  $\mathbf{i1}$  (*cis* form) and  $\mathbf{i6}$  (*trans* form), respectively. Note that the reaction energies to form the *cis* and *trans* forms are too close, within  $1 \text{ kJ mol}^{-1}$ , to make a definite determination when compared to the experimental values for the formation of *cis*, *trans*, or both isomers. It should be noted that based on the results from the 3,3,3-D3-propylene experiment alone, the hydrogen release could also account for the formation of D3-2-phenylpropene ( $\text{C}_6\text{H}_5\text{CD}_3\text{CCH}_2$ ;  $\mathbf{p6}$ ) formed from  $\mathbf{i2}$ . Here, the theoretically predicted reaction energy falls within the range of the experimentally determined ones. Finally, the energetics of the experimentally observed methyl loss pathway (R2) of  $-74 \pm 14 \text{ kJ mol}^{-1}$  agree very well with the formation of the styrene molecule ( $\mathbf{p5}$ ). The mechanism can involve either a unimolecular decomposition of  $\mathbf{i2}$  and/or  $\mathbf{i6}$ .

To summarize, a comparison of the experimental and calculated reaction energies together with the results from scattering experiments with (partially) deuterated reactants suggests the following channels. First, reactions with 1,1,2-D3-propylene verify the formation of D3-3-phenylpropene ( $\text{H}_2\text{CCDCD}_2\text{C}_6\text{H}_5$ ;  $\mathbf{p3}$ ); the hydrogen atom is lost from the former methyl group of the propylene reactant. Secondly, reactions with 3,3,3-D3-propylene can account for the formation of *cis*- and/or *trans*-1-phenylpropene ( $\text{CD}_3\text{CHCHC}_6\text{H}_5$ ;  $\mathbf{p1/p2}$ ) and/or D3-2-phenylpropene ( $\text{C}_6\text{H}_5\text{CD}_3\text{CCH}_2$ ;  $\mathbf{p6}$ ). In these pathways, the hydrogen atom is released from the vinyl group. Third, we provided evidence on the formation of styrene ( $\mathbf{p5}$ ) plus the methyl radical. As verified experimentally, all pathways involve indirect reaction dynamics *via* complexes with lifetimes longer than their rotational periods. Further, all intermediates leading to atomic hydrogen and methyl loss involve tight exit transition states as predicted experimentally and verified in the electronic structure calculations. Compared to an earlier investigation of this system at elevated collision energies up to  $194 \text{ kJ mol}^{-1}$ ,<sup>16</sup> the reduced collision energy of less than  $49 \text{ kJ mol}^{-1}$  leads to an enhanced lifetime of the reaction intermediates (long lived at  $49 \text{ kJ mol}^{-1}$  *versus* oscillating complex model at elevated collision energies). Further, the detection of the methyl loss pathway in the present study can be attributed to a phenyl radical beam with number densities enhanced by almost one order of magnitude

compared to the previous study utilizing a pyrolytic source,<sup>16</sup> and/or a less favorable formation of **i2**, and/or a shorter lifetime of **i1**, which limits the hydrogen migration to **i6** and successive methyl group loss at higher collision energies.

We also conducted RRKM calculations of reaction rate constants followed by computations of product branching ratios on the C<sub>9</sub>H<sub>11</sub> surface including all considered reaction steps shown on Fig. 11 at collision energies varied within 6–200 kJ mol<sup>-1</sup>, where the lowest collision energy corresponds to the reaction entrance barrier to form **i1**. All product branching ratios are collected in Table 2. First, in order to evaluate relative contributions of the two entrance reaction channels, C<sub>6</sub>H<sub>5</sub> + C<sub>3</sub>H<sub>6</sub> → **i1**/**i2**, we calculated their thermal rate constants at  $T = 2E_{\text{col}}/3R$ , *i.e.*, considering the collision energy as the average kinetic energy corresponding to a certain temperature and using this temperature in the rate constant calculations based on canonical transition state theory for a bimolecular reaction. Note that the canonical TST calculations were employed only for the bimolecular entrance channel thermal rate constants. Although more accurate results can be achieved by computing bimolecular reaction cross sections as functions of collision energy, the branching ratios of the two entrance channels evaluated as  $k_1/k$  and  $k_2/k$ , where  $k_1$  and  $k_2$  are the rate constants for the formation of **i1** and **i2**, respectively, and  $k = k_1 + k_2$  is the total rate constant for the phenyl addition to propylene, appeared to be not very sensitive to  $T$  and thus  $E_{\text{col}}$ . Also, the isomerization between **i1** and **i2** is faster than any of the dissociation processes and therefore, we expect that the canonic approximation used for the relative yields of the entrance channels should not affect the product branching ratios significantly. We found that the formation of the **i1** adduct is a significantly more favorable process as compared to the formation of **i2**, accounting for more than 80% of the reaction flux at all studied collision energies. Note that with an increase of the collision energy, the contribution of **i2** slightly increases, from 0% at  $E_{\text{col}} = 6$  kJ mol<sup>-1</sup> to 16.5% at  $E_{\text{col}} = 200$  kJ mol<sup>-1</sup>. This indicates that at the considered collision energies the product formation mostly results from rearrangements/dissociations involving the **i1** intermediate formed by the phenyl radical addition to the C1 carbon of propylene.

The major reaction products predicted by calculations of the product branching ratios include styrene (**p5**) plus methyl radical and 3-phenylpropene (**p3**) plus hydrogen atom with relative yields varying significantly with the collision energy and accounting together for more than 90% of the total product yield. The production of *cis*-1-phenylpropene (**p1**) and 2-phenylpropene (**p6**) give relatively small contributions of 0.1–5% and ~1%, respectively, whereas the yields of all other products, including indane (**p4**) and other bicyclic structures (**p8** and **p9**), are found to be negligible. At low collision energies the formation of styrene significantly prevails over that of 3-phenylpropene, for instance, their branching ratio is 87:11 at  $E_{\text{col}} = 20$  kJ mol<sup>-1</sup>. However, at  $E_{\text{col}} \sim 80$  kJ mol<sup>-1</sup> their yields become close, 50:46, and with the further collision energy increase 3-phenylpropene (**p3**) takes over and becomes the most important reaction product. At  $E_{\text{col}} = 200$  kJ mol<sup>-1</sup>, the **p5**/**p3** branching ratio is calculated to be 22:72. In addition, we carried out branching ratio calculations with **i1** or **i2** being exclusive initial intermediates, *i.e.* with the entrance channel branching ratios of 100/0 and 0/100, respectively. The results shown in Table 2 confirm that the branching ratios of **p5** and **p3** are not very sensitive to the choice of the initial intermediate. Only at the highest collision energies considered, 180–200 kJ mol<sup>-1</sup>, the relative yield of **p5** + CH<sub>3</sub> increases by 8–10% if the reaction starts solely from **i2** as compared to that when it starts from **i1**, whereas the yield of **p3** + H respectively decreases.

Our kinetic analysis shows that 3-phenylpropene is nearly exclusively produced *via* the one-step **i1** → **p3** + H process, whereas the contributions from the two-step **i1** → **i4**/**i5** → **p3** + H mechanisms are negligible. Styrene **p5** is exclusively formed directly by CH<sub>3</sub> loss from **i2**, where **i2** itself can be produced both *via* the **i1** → **i3** → **i2** rearrangement and straight from the reactants. The contribution of the **i1** → **i6** → **p5** + CH<sub>3</sub> pathway was found to be negligible. The increase of the product yield of 3-phenylpropene parallel to the decrease of the styrene production with increasing collision energy can be attributed only to the competition between the direct H loss, **i1** → **p3** + H, and the fast isomerization of **i1** to **i2** *via* the bicyclic intermediate **i3**; **i2** would further dissociate to styrene

**Table 2** Calculated product branching ratios (%) under single-collision conditions at various collision energies of 0–200 kJ mol<sup>-1</sup>

Product	Collision energy, kJ mol <sup>-1</sup>										
	6.3	20	40	60	80	100	120	140	160	180	200
C <sub>6</sub> H <sub>5</sub> + C <sub>3</sub> H <sub>6</sub> → <b>i1</b>	100.0	87.5	85.4	84.6	84.3	84.0	83.8	83.7	83.6	83.6	83.5
C <sub>6</sub> H <sub>5</sub> + C <sub>3</sub> H <sub>6</sub> → <b>i2</b>	0.0	12.5	14.6	15.4	15.7	16.0	16.2	16.3	16.4	16.4	16.5
<b>p5</b> + CH <sub>3</sub> <sup>a</sup>	95.2	87.0	72.8	60.0	49.8	41.8	36.0	31.4	27.5	24.7	22.4
		(87.0–87.1)	(72.8–72.9)	(59.9–60.1)	(49.8–50.3)	(41.6–42.7)	(35.7–37.7)	(30.8–34.2)	(26.7–31.9)	(23.5–31.0)	(20.7–30.9)
<b>p3</b> + H <sup>a</sup>	3.3	10.8	24.1	36.1	45.6	53.1	58.6	63.0	66.6	69.2	71.5
		(10.8–10.8)	(24.1–24.0)	(36.1–35.9)	(45.6–45.2)	(53.3–52.3)	(58.9–56.9)	(63.5–60.2)	(67.4–62.4)	(70.4–63.2)	(73.1–63.2)
<b>p1</b> + H	0.4	1.0	2.0	2.8	3.5	3.9	4.3	4.5	4.7	4.9	5.0
<b>p6</b> + H	1.2	1.1	1.1	1.1	1.1	1.1	1.0	1.0	1.0	0.9	0.9
<b>p8</b> + CH <sub>3</sub>	0.0	0.0	0.0	0.0	0.0	0.0	0.0	0.0	0.0	0.0	0.0
<b>p9</b> + H	0.0	0.0	0.0	0.0	0.0	0.0	0.0	0.0	0.0	0.0	0.0
<b>p4</b> + H	0.0	0.0	0.0	0.0	0.0	0.1	0.1	0.1	0.2	0.2	0.2
<b>p7</b> + H	0.0	0.0	0.0	0.0	0.0	0.0	0.0	0.0	0.0	0.0	0.0
<b>p2</b> + H	0.0	0.0	0.0	0.0	0.0	0.0	0.0	0.0	0.0	0.0	0.0

<sup>a</sup> Numbers in parameters show branching ratios calculated assuming **i1** (the first number) or **i2** (the second number) as the exclusive initial adduct.

plus methyl. At low collision energies, the  $\mathbf{i1} \rightarrow \mathbf{p3} + \text{H}$  process is significantly slower than the  $\mathbf{i1} \rightarrow \mathbf{i3} \rightarrow \mathbf{i2}$  rearrangement; for instance, at  $E_{\text{col}} = 6 \text{ kJ mol}^{-1}$  the rate constant for  $\mathbf{i1} \rightarrow \mathbf{p3} + \text{H}$  is a few orders of magnitude lower than that for  $\mathbf{i1} \rightarrow \mathbf{i3}$ . In this case, the initially produced adduct  $\mathbf{i1}$  tends to quickly isomerize to  $\mathbf{i2}$ , which then exclusively dissociates to styrene +  $\text{CH}_3$ , as the other isomerizations/dissociations of  $\mathbf{i2}$  are found to be insignificant. The rise of  $E_{\text{col}}$  rapidly increases the rate constant for  $\mathbf{i1} \rightarrow \mathbf{p3} + \text{H}$ ; for instance, at  $E_{\text{col}} = 200 \text{ kJ mol}^{-1}$  it becomes less than one order of magnitude lower than that for  $\mathbf{i1} \rightarrow \mathbf{i3}$ . Meanwhile, the  $\mathbf{i1} \leftrightarrow \mathbf{i3} \leftrightarrow \mathbf{i2}$  equilibrium tends to shift towards  $\mathbf{i1}$ , resulting in the reaction flux going predominantly towards the formation of 3-phenylpropene + H. The increase of the yield of *cis*-1-phenylpropene ( $\mathbf{p1}$ ) with  $E_{\text{col}}$  (from 0.4 to 5% within the 6–200  $\text{kJ mol}^{-1}$  range) is also attributed to the shift of the  $\mathbf{i1} \leftrightarrow \mathbf{i3} \leftrightarrow \mathbf{i2}$  equilibrium towards  $\mathbf{i1}$ , which reduces the consumption of  $\mathbf{i1}$  via the  $\mathbf{i1} \rightarrow \mathbf{i3} \rightarrow \mathbf{i2} \rightarrow \mathbf{p5} + \text{CH}_3$  mechanism; the competition between the  $\mathbf{i1} \rightarrow \mathbf{p1} + \text{H}/\mathbf{p3} + \text{H}$  reactions, in fact, does not play any significant role in this case.

Finally, the branching ratios between the methyl loss channel and atomic hydrogen loss channel were derived from the experimental data are  $68 \pm 16\% : 32 \pm 10\%$ . This gives a good match to the overall branching ratios calculated by the RRKM theory of 69.6% : 30.4% for the methyl group versus hydrogen atom loss at a collision energy of 45  $\text{kJ mol}^{-1}$ . Considering experimental results from studies of this system at higher collision energies of 130–193  $\text{kJ mol}^{-1}$ , theory predicts decreasing branching ratios of down to 20–30%. If we transmit that back into an expected observable signal, we can see that it is below the detection threshold which confirms the accuracy of the RRKM theory on the branching ratio for this system. This agrees very well with our experimental estimate of less than 10% of the methyl group loss at elevated collision energies.<sup>16</sup>

## 6. Conclusion

The crossed molecular beams reactions of the phenyl radical with propylene together with its partially deuterated reactants was conducted at collision energies of  $\sim 45 \text{ kJ mol}^{-1}$ . Experimental data suggest indirect scattering dynamics via  $\text{C}_9\text{H}_{11}$  collision complexes resulting into two competing channel: the methyl group loss leading to styrene ( $\text{C}_6\text{H}_5\text{C}_2\text{H}_3$ ) and the atomic hydrogen loss forming  $\text{C}_9\text{H}_{10}$  isomers *cis/trans* 1-phenylpropene ( $\text{CH}_3\text{CHCHC}_6\text{H}_5$ ) and 3-phenylpropene ( $\text{C}_6\text{H}_5\text{CH}_2\text{C}_2\text{H}_3$ ). Fractions of the methyl versus hydrogen loss channels of  $68 \pm 16\% : 32 \pm 10\%$  were derived experimentally, which agrees nicely with RRKM theory. As the collision energy rises to 200  $\text{kJ mol}^{-1}$ , the contribution of the methyl loss channel decreases sharply to typically 25%; the decreased importance of the methyl group loss channel was also demonstrated in previous crossed beam experiments conducted at elevated collision energies of 130–193  $\text{kJ mol}^{-1}$ .<sup>16</sup> The presented work highlights the interesting differences of the branching ratios with rising collision energies in the reaction dynamics of phenyl radicals with unsaturated hydrocarbons related to combustion processes. The facility of forming styrene, a common molecule found in combustion against the elusiveness of forming the cyclic indane molecule demonstrates the need to continue to explore the potential surfaces

through the combinative single collision experiment and electronic structure calculations.

## Acknowledgements

This work was supported by the US Department of Energy, Basic Energy Sciences (DE-FG02-03ER15411 to the University of Hawaii and DE-FG02-04ER15570 to Florida International University).

## References

- M. Kamphus, M. Braun-Unkoff and K. Kohse-Hoinghaus, *Combust. Flame*, 2008, **152**, 28–59.
- J. J. Newby, J. A. Stearns, C.-P. Liu and T. S. Zwier, *J. Phys. Chem. A*, 2007, **111**, 10914–10927.
- Y. Li, Z. Tian, L. Zhang, T. Yuan, K. Zhang, B. Yang and F. Qi, *Proc. Combust. Inst.*, 2009, **32**, 647–655.
- Y. Li, L. Zhang, Z. Tian, T. Yuan, J. Wang, B. Yang and F. Qi, *Energy Fuels*, 2009, **23**, 1473–1485.
- Y. Li, L. Zhang, Z. Tian, T. Yuan, K. Zhang, B. Yang and F. Qi, *Proc. Combust. Inst.*, 2009, **32**, 1293–1300.
- P. Lindstedt, L. Maurice and M. Meyer, *Faraday Discuss.*, 2001, **119**, 409–432; discussion pp. 445–459.
- Y. Li, L. Zhang, T. Yuan, K. Zhang, J. Yang, B. Yang, F. Qi and C. K. Law, *Combust. Flame*, 2010, **157**, 143–154.
- S. P. Verevkin, V. N. Emel'yanenko, A. A. Pimerzin and E. E. Vishnevskaya, *J. Phys. Chem. A*, 2011, **115**, 1992–2004.
- E. Pousse, Z. Y. Tian, P. A. Glaude, R. Fournet and F. Battin-Leclerc, *Combust. Flame*, 2010, **157**, 1236–1260.
- H. Richter and J. B. Howard, *Prog. Energy Combust. Sci.*, 2000, **26**, 565–608.
- M. Frenklach, *Phys. Chem. Chem. Phys.*, 2002, **4**, 2028–2037.
- X. Gu, F. Zhang, Y. Guo and R. I. Kaiser, *Angew. Chem., Int. Ed.*, 2007, **46**, 6866–6869.
- X. Gu, F. Zhang and R. I. Kaiser, *J. Phys. Chem. A*, 2009, **113**, 998–1006.
- F. Zhang, X. Gu and R. I. Kaiser, *J. Chem. Phys.*, 2008, **128**, 084311–084315.
- X. Gu and R. I. Kaiser, *Acc. Chem. Res.*, 2009, **42**, 290–302.
- F. Zhang, X. Gu, Y. Guo and R. I. Kaiser, *J. Phys. Chem. A*, 2008, **112**, 3284–3290.
- J. Park, G. J. Nam, I. V. Tokmakov and M. C. Lin, *J. Phys. Chem. A*, 2006, **110**, 8729–8735.
- R. I. Kaiser, P. Maksyutenko, C. Ennis, F. Zhang, X. Gu, S. P. Krishtal, A. M. Mebel, O. Kostko and M. Ahmed, *Faraday Discuss.*, 2010, **147**, 429–478.
- NIST Chemistry WebBook*, ed. P. J. Linstrom and W. G. Mallard, NIST Standard Reference Database Number 69.
- X. B. Gu, Y. Guo, E. Kawamura and R. I. Kaiser, *Rev. Sci. Instrum.*, 2005, **76**, 083111–083116.
- Y. Guo, X. Gu, E. Kawamura and R. I. Kaiser, *Rev. Sci. Instrum.*, 2006, **77**, 034701–034709.
- M. Vernon, *PhD thesis*, University of California, Berkley, 1981.
- D. Krajnovich, F. Huisken, Z. Zhang, Y. R. Shen and Y. T. Lee, *J. Chem. Phys.*, 1982, **77**, 5977–5989.
- A. D. Becke, *J. Chem. Phys.*, 1992, **97**, 9173–9177.
- A. D. Becke, *J. Chem. Phys.*, 1992, **96**, 2155–2160.
- A. D. Becke, *J. Chem. Phys.*, 1993, **98**, 5648–5652.
- C. Lee, W. Yang and R. G. Parr, *Phys. Rev. B*, 1988, **37**, 785–789.
- A. G. Baboul, L. A. Curtiss, P. C. Redfern and K. Raghavachari, *J. Chem. Phys.*, 1999, **110**, 7650–7657.
- L. A. Curtiss, K. Raghavachari, P. C. Redfern, A. G. Baboul and J. A. Pople, *Chem. Phys. Lett.*, 1999, **314**, 101–107.
- L. A. Curtiss, K. Raghavachari, P. C. Redfern, V. Rassolov and J. A. Pople, *J. Chem. Phys.*, 1998, **109**, 7764–7776.
- M. J. Frisch, *et al.*, *GAUSSIAN 98 (Revision A.11)*, 1998.
- H.-J. Werner, *et al.*, *MOLPRO, version 2006.1*, 2006.
- H. Eyring, S. H. Lin and S. M. Lin, *Basic Chemical Kinetics*, Wiley, New York, 1980.
- P. J. Robinson and K. A. Holbrook, *Unimolecular Reactions*, Wiley, New York, 1972.
- J. I. Steinfeld, J. S. Francisco and W. L. Hase, *Chemical Kinetics and Dynamics*, Prentice Hall, Englewood Cliffs, NJ, 1999.